Synergistic action of actinoporin isoforms from the same sea anemone species assembled into functionally active heteropores.

Esperanza Rivera-de-Torre[1], Sara García-Linares[1], Jorge Alegre-Cebollada[2], Javier Lacadena[1], José G. Gavilanes[1] and Álvaro Martínez-del-Pozo[1]

From the [1]Departamento de Bioquímica y Biología Molecular I, Facultades de Química y Biología, Universidad Complutense, 28040 Madrid, Spain.
[2]Centro Nacional de Investigaciones Cardiovasculares Carlos III (CNIC), Madrid, Spain.

Running title: *Functionally active actinoporin heteropores*

To whom correspondence should be addressed: José G. Gavilanes (ppgf@bbm1.ucm.es) and Álvaro Martínez-del-Pozo (alvaromp@quim.ucm.es), Departamento de Bioquímica y Biología Molecular I, Facultad de Química, Universidad Complutense, 28040 Madrid, Spain, Telephone: 34 91 3944158; FAX: 34 91 3944159.

Keywords: pore-forming-toxin, sticholysin, equinatoxin, erythrocyte, toxin, oligomerization, cross-linking, lysis, lipid-protein interaction, ion channel.

ABSTRACT

Among the toxic polypeptides secreted in the venom of sea anemones, actinoporins are pore forming toxins whose toxic activity relies on the formation of oligomeric pores within biological membranes. Intriguingly, actinoporins appear as multigene families which give rise to many protein isoforms in the same individual displaying high sequence identities but large functional differences. However, the evolutionary advantage of producing such similar isotoxins is not fully understood. Here, using sticholysins I and II (StnI and StnII) from the sea anemone *Stichodactyla helianthus*, it is shown that actinoporin isoforms can potentiate each other's activity. Through hemolysis and calcein releasing assays, it is revealed that mixtures of StnI and StnII are more lytic than equivalent preparations of the corresponding isolated isoforms. It is then proposed that this synergy is due to the assembly of heteropores since (i) StnI and StnII can be chemically cross-linked at the membrane and (ii) the affinity of sticholysin mixtures for the membrane is increased with respect to any of them acting in isolation, as revealed by isothermal titration calorimetry experiments. These results help to understand the multigene nature of actinoporins and may be extended to other families of toxins that require oligomerization to exert toxicity.

Actinoporins constitute a family of toxic proteins produced by different sea anemone species as single polypeptide chains of around 175 amino acids. They show basic isoelectric point values and are usually cysteineless (1-4). Actinoporins belong to a much larger group of widely distributed proteins, known as *pore forming toxins* (PFT), whose toxic activity relies on the formation of pores within biological membranes (5-9). All PFTs show a very similar dual behavior by which they remain mostly monomeric and stably folded in aqueous solution but become oligomeric integral proteins when encountering membranes (2-4,10-23).

The incorporation of actinoporins into the membrane largely depends on lipid bilayer composition and membrane physicochemical state (18,24-29). Both factors influence the conformational changes occurring during the transition from the water media to the inserted states of the protein (30,31). Thus, high affinity recognition of sphingomyelin (SM) is crucial for specific attachment to a membrane but the subsequent effects observed also depend on the physical properties derived from its particular

composition and not only from its SM content (23,32). In fact, although still controversial, the presence of cholesterol and coexistence of different phases in the membrane seem to be important factors, if not for binding, at least for the final formation of the pore (23,28,29,32-36).

Actinoporins have been isolated from more than 20 different sea anemone species (1,3,37-41) in agreement with their rather ubiquitous distribution within the *Actinaria* order (1). They display high sequence identities (between 60% and 80%) and appear as multigene families, giving rise to many protein isoforms within the same individual (42-46). Despite the small number of amino acid changes between them, actinoporin isoforms usually result in substantial functional differences in terms of solubility and lytic activity (38,45,47-51), as exemplified by StnI and StnII, produced by *Stichodactyla helianthus*, and also two of the best characterized actinoporins (3,4,20,22,24,47-50,52).

The reason why a single anemone produces several isoforms of actinoporins in its venom is still not fully understood. One possible explanation would be to expand the range of prey susceptible of being attacked (53). Such a strategy would extend and modulate the range of sea anemones action. It has even been proposed an analogy with immunoglobulins which suggests that sea anemone tentacles would produce many actinoporins isoforms because they would represent the embryo of a rudimentary defense system (45). However, so far the possibility that these different isoforms show synergistic activity has not been explored. This possibility is interesting since it would lead to more efficient venoms. The results presented here not only prove that StnI and StnII potentiate their lytic activity when they act together, but also indicate that they can establish functional heteropores, suggesting that actinoporins have a more deeply regulated physiological mode of action than previously believed.

EXPERIMENTAL PROCEDURES

Materials - 1,2-dioleoyl-sn-glycero-3-phosphocholine (DOPC), cholesterol (Chol), and porcine brain sphingomyelin (SM) were obtained from Avanti Polar Lipids. Disuccinimidyl suberate (DSS) was purchased from Pierce (Thermo Scientific). The preparation of the cDNA coding for StnI, StnII and the six His tagged version of StnII (6HStnII), as well as the production and purification of the three different proteins, has been described before (30,50,54). Homogeneity of all protein samples used was analyzed by 0.1% (w/v) SDS/12-15% (w/v) PAGE performed in standard conditions (55) and amino acid analysis after acid hydrolysis of the proteins (5.7 M HCl, 24 h, 110°C). These amino acid analyses were performed on a Biochrom 20 automatic analyzer (Pharmacia). All protein batches used were also previously characterized in terms of recording their far-UV circular dichroism (CD) spectra on a Jasco 715 spectropolarimeter, also as described (20,21,56,57).

Hemolysis - Hemolysis assays were performed in 96-multiwell plates as previously described (30,50). Briefly, erythrocytes from heparinized sheep blood were washed in 10 mM Tris buffer, pH 7.4, containing 145 mM NaCl, to a final OD_{655} of 0.5 when mixing equal volumes of the cell suspension and buffer. The hemolysis was followed as a decrease in OD_{655} after addition of the erythrocyte suspension to different final concentrations of protein. An Expert 96 microplate reader (Asys Hitech, GmbH, Eugendorf, Austria) was employed to measure OD_{655}. The value obtained with 0.1% (w/v) Na_2CO_3 was considered as 100% hemolysis.

Lipid vesicle preparation - DOPC:SM:Chol (1:1:1) phospholipid vesicles were prepared as previously described (20,23,58). A phospholipid (0.1–1.0 mg) solution in 2:1 (v/v) chloroform/methanol was dried under a flow of nitrogen, and the dry film obtained was used to prepare a lipid dispersion by adding 0.5-2.0 mL of Tris/NaCl (10 mM Tris–HCl, pH 7.4, 140 mM NaCl), briefly vortex-mixing, and incubating for 1 h at 37 ºC. This suspension of multilamellar vesicles was further subjected to five cycles of extrusion at 37 ºC through polycarbonate filters (100-nm pore size) to obtain a homogeneous population of unilamellar vesicles.

Calcein leakage assays - Calcein-entrapped DOPC:SM:Chol (1:1:1) large unilamellar vesicles (LUVs) were prepared as

described (23) by extrusion through 100 nm filters (Nucleopore, Whatman) at 37 °C. Briefly, the desired lipids were mixed and dried under a stream of nitrogen. The lipids were re-dissolved in chloroform and dried again before removal of any traces of remaining solvent in vacuum for 60 min. Prior to extrusion, the dry lipid films were hydrated for one hour at 37 °C in Tris buffer (10 mM Tris, 140 mM NaCl, 0.5 mM EDTA pH 7.4), containing 100 mM calcein. The total lipid concentration was 1.25 mM. LUVs were separated from non-entrapped calcein by gel filtration on Sephacryl S200HR. These LUVs were used for permeabilization studies within 24 h. Phospholipid concentration was determined from phosphorous measurement (59) after elution of vesicles during isolation. The concentration of LUV phospholipids and protein during calcein leakage experiments were about 7.5 μM and 1-80 nM, respectively. Emission at 550 nm was followed at 23 °C as a function of time (excitation at 480 nm). Fluorescence emission was measured with an SLM Aminco 8000 spectrofluorimeter. To ensure that no major spontaneous leakage occurred, the emission was measured for each sample during 5 min before addition of toxin. A steady signal level, indicating intact vesicles, was observed for all samples. Maximum calcein release was determined upon LUV disintegration induced by 10% Triton X-100.

Cross-linking experiments - Cross-linking was performed essentially as described before (60). DSS was used as the cross-linking reagent in a reaction which was performed by adding a small aliquot of a concentrated freshly prepared cross-linker solution to the protein sample, at the required concentrations. Protein (wild-type StnI and a 6 x His tagged version of StnII [6HStnII]) (50) and vesicle mixtures were prepared in 15 mM MOPS, pH 7.4, containing 50 mM NaCl, at the following final molar concentrations: 2.0 μM StnI, 0.5 μM 6HStnII, 0.1 μM (lipid concentration) DOPC:SM:Chol (1:1:1) phospholipid vesicles, and 0.04 μM DSS. The final concentration of each protein employed was in this case independent of the presence or not of the other actinoporin. A second set of cross-linking experiments were made with mixtures containing a constant concentration of 6HStnII and increasing amounts of StnI up to a StnI:6HStnII molar ratio of 95:5. The cross-linker was dissolved in dimethyl sulfoxide (DMSO). The protein-lipid reaction mixtures were incubated at 37 ºC for 1 hour, then the cross-linker was added and kept for 30 minutes at room temperature, and finally the mixtures were quenched for 15 min by adding an aliquot of the same buffer but containing 50 mM Lys. After addition of the corresponding electrophoresis loading buffer to each aliquot, they were boiled for 20 min in the presence of 0.5% (v/v) β-mercaptoethanol and the cross-linked products were analyzed by SDS-PAGE following standard procedures (55). Western immunoblotting was used to detect 6HStnII using a mouse monoclonal anti-poly-Histidine-peroxidase antibody from Sigma-Aldrich.

Protein binding to lipid vesicles - Binding was measured using isothermal titration calorimetry (ITC) as described before (21,30,61), using a VP-ITC calorimeter (MicroCal). Briefly, protein solutions at 1.5-10.0 μM concentration were titrated by injection of 10 or 20 μL aliquots of lipid suspensions (phospholipid concentration: 0.85-5.00 mM). Binding isotherms were adjusted to a model were the protein binds to the membrane involving “n” lipid molecules (30).

RESULTS

StnI and StnII show synergistic hemolytic activity - A hemolysis experiment was designed to study the potential formation of StnI/StnII heteropores and its functional consequences. Within this idea, sheep erythrocyte hemolysis was assayed in the presence of isolated StnI or StnII at different concentrations or for a mixture of StnI:StnII at 80:20 constant molar ratio (Fig. 1). This experiment was so designed given the lower hemolytic activity of StnI. Inspection of results shown in Fig. 1 reveal how the mixture produced higher hemolysis rates than that one resulting from the arithmetical combination of the corresponding values obtained with the individual proteins.

In order to evaluate the specificity of this observation two different StnII mutants were employed as controls. First, the same experiment as that described in Fig. 1 was made using StnII A10PS28P instead of the wild-type protein. This mutant has been previously described as retaining its full membrane binding activity but showing a highly diminished pore forming ability due to its

inability to extend the needed α helical stretch (30). As shown in Fig. 2A, even though the mutant was completely unable to lyse the erythrocytes within the full concentration range assayed, the mixture still produced higher hemolysis rates than those ones resulting from the arithmetical combination of the corresponding values obtained with the individual proteins (wild-type StnI and A10PS28P StnII at a 80:20 ratio).

In the second control experiment performed, the StnII mutant used was Y111N. In this StnII variant a key residue of the so called phosphocholine (POC)-binding site has been replaced rendering a protein which cannot bind to the membrane and, therefore, shows a dramatically reduced hemolytic activity (30,54). It can be seen how in this case (Fig. 2B) the synergic effect of StnII is not observed.

Overall, the three sets of experiments suggest not only the existence of synergistic action between both actinoporin isoforms, StnI and StnII, but also that this synergy seems to occur at the membrane binding step of the pore formation mechanism

StnI and StnII show synergistic lytic activity towards lipid model vesicles – Erythrocytes are a rather complex model system to study protein-lipid interactions and assembly of pores at the membrane. Therefore, an experiment was designed to study leakage of calcein-containing DOPC:SM:Chol (1:1:1) phospholipid vesicles upon addition of different actinoporin concentrations. This type of vesicles represents one of the standard models most widely used to characterize StnI and StnII pore formation behavior (18,20,23,28,30,54,62). As it can be observed in Fig. 3, the results obtained were similar to those ones corresponding to the hemolysis assays. The mixture of StnI and StnII produced higher calcein release rates than that one resulting from the arithmetical combination of the corresponding values obtained with the individual proteins.

StnI and StnII can be cross-linked in the presence of lipid membranes - The results obtained from both sets of activity experiments, hemolysis and calcein release assays, show that StnI and StnII display synergistic activity. One explanation for this synergy would be the formation of active StnI/StnII heteropores. If this was the case, molecules of both different proteins studied should be in enough proximity as to be cross-linked using a short bifunctional reagent such as DSS (spacer arm: 1.1 nm), which reacts against exposed primary amines. Consequently, mixtures of StnI and StnII were incubated in the presence or absence of DOPC:SM:Chol (1:1:1) phospholipid vesicles and then DSS was added, following a standard protocol (63). The resulting mixture of proteins was analyzed by means of SDS-PAGE followed by Western blotting and immunodetection. For this purpose, instead of the wild type protein, a 6xHis tagged version of StnII (6HStnII) was employed. This protein has been described to retain the general features and molecular mechanism of wild-type StnII (50,64). This 6HStnII variant shows two advantages for cross-linking experiments. First, the presence of the N-terminus polyHis tag shifts its electrophoretic mobility to the point that it can be unequivocally distinguished from wild-type StnI (50). Second, it can be identified by an anti-poly-His antibody without cross-reactivity from StnI (18). Therefore, the results presented in blots of Figs. 4 and 5 reveal only the presence of 6HStnII, independently of the amount of StnI present.

In the absence of vesicles, only 6HStnII is detected in lanes 1 and 2 of Fig. 4 in spite of the presence of a four-fold higher concentration of StnI or the previous addition, or not, of the cross-linking agent. Lanes 3 and 4 show the same set of results, cross-linked or not, but this time after incubation of both proteins with DOPC:SM:Chol (1:1:1) vesicles. Thus, again, in the absence of DSS, no other band but that one corresponding to monomeric 6HStnII was observed (lane 3). However, when the cross-linker was present new bands of different electrophoretic mobility were evident (Fig.4, lane 4). At least two of these bands were not observed if 6HStnII (lane 5) or StnI (lane 6) were the only proteins present. Therefore, they can only correspond to hetero-oligomers made of 6HStnII and wild-type StnI, the only situation that would explain their immunodetection by the anti-poly-His antibody altogether with their singular electrophoretic mobility. It has been well determined that the presence of the six His tag at

the N-terminal end of sticholysins has a deep impact on their electrophoretic mobility (50)

In order to show further evidence of the assembly of StnI and 6HStnII into cross-linkable heteropores, the titration experiment shown in Fig. 5 was performed. Again, in these conditions, in the absence of vesicles, only 6HStnII was detected in lane 1. However, when crosslinker and vesicles were present, 6HStnII cross-linked oligomers could be detected (lane 2). In fact, the observed distribution pattern is very similar to that one reported before for EqtII under almost identical conditions (25,65). As shown in lanes 2 to 5, upon increasing the StnI:6HStnII ratio the appearance of the bands corresponding to cross-linked proteins is increasingly evident altogether with a decrease of the monomeric 6HStnII species. This second set of results does not only confirm the presence of cross-linkable heteropores on the bilayer but also its marked protein concentration and StnI/6HStnII ratio dependence. The presence of other hetero-oligomers of lower electrophoretic mobility is also detected but, given the inherent influence of the DSS reaction on band electrophoretic mobility and sharpness (60), it is not possible to assign specific stoichiometries. We also used Coomassie staining to analyze the results of crosslinking. Comparing with the western blot results, we found that the lower mobility heteroligomer bands at around 40KDa that become apparent at higher StnI:6HStnII ratios have a lower reactivity against the anti-His antibody, in agreement with the lower content of His-tags in the heteroligomers.

In summary, this set of experiments allowed to conclude that, in the presence of membranes, actinoporins StnI and StnII are closely enough as to be cross-linked by a short crosslinking agent, suggesting that heteropores of StnI and StnII are formed.

Mixtures of StnI and StnII show increased membrane affinity – The actinoporins pore-formation mechanism has been thoroughly studied although some of its details are still subject of dispute (17,32,66-70). In a simplified version of this mechanism, two different steps can be distinguished: First, the protein binds to the membrane and, second, assembles into a functional oligomeric pore (18,30). Within the context of this simplified picture, it can be assumed that binding assays by isothermal titration calorimetry (ITC) measure the affinity of the proteins to the membrane (30). As it can be observed in Fig. 6, the affinity of StnI for DOPC:SM:Chol (1:1:1) phospholipid vesicles is lower than that one corresponding to StnII (Table 1). In terms or relative membrane binding affinity (RMB), StnII binding to the vesicles is four fold-higher, a result that is good enough by itself to explain the long-known differences in terms of hemolytic and calcein-leakage activities between StnI and StnII (26,71).

In order to explore whether improved binding could contribute to the synergistic lytic activity shown by sticholysins, we performed ITC binding experiments in which a total actinoporin concentration was fixed but different StnI/StnII molar ratios were assayed (Fig. 7). Quite surprisingly, the binding affinity of mixtures of StnI and StnII was always higher than for any of the two actinoporins acting in isolation. This effect was already detected in the presence of trace amounts (1.0%) of StnII and correlated with increased RMB (Fig. 7 and Table 1). It is difficult to conceive how the binding affinity could increase without direct interaction between StnI and StnII. Hence, the ITC experiments lend additional support to the hypothesis that StnI and StnII can assemble into functional heteropores, leading to synergistic lytic activity.

Finally, given the large effect on affinity of only traces of StnII in the mixtures, it was studied if this increase in binding affinity was directly correlated with an enhancement of function. As can be seen in Fig. 8, just 1.0% of StnII in the mixtures was enough to dramatically improve their hemolytic activity, as revealed by the hemolysis assays performed with different StnI:StnII (99:1) mixtures over a 1-10 nM concentration range (Fig. 8).

DISCUSSION

Sea anemones produce a wide variety of toxic compounds that are mainly stored in their nematocysts (72). Among them, actinoporins constitute a well-studied family of toxic pore-forming proteins (3,4,70). It has been long time known that individual sea anemones species produce many different actinoporins isoforms

which, indeed, are very differently represented in terms of the amount present in their venomous secretions. In this regard, actinoporins represent a well-established example of a multigenic protein family (38,39,43,45,46,51,73). They are not, however, the only example of toxic pore-forming multigene protein families (74), suggesting that the results shown now could be of larger significance and not only restricted to the actinoporins family. In fact, it has been very recently suggested that the pore responsible for damaging michondria during apoptosis could be made of hetero-oligomers of the Bax and Bak proteins (75). The natural biological function of this genetic multiplicity is indeed far from being understood. Regarding the actinoporins family, it has been proposed that the existence of multiple isoforms would broaden the range of possible prey for a given species (38,39,43,45,46,51,73). In this regard, actinoporins might be similar to immunoglobulins, which require a plethora of highly diverse genes to counteract foreign antigens (45).

Here, we propose a complementary hypothesis to explain the evolutionary advantage of multigenic actinoporins: formation of mixed functional pores. This mechanism would enable a much wider and finely tuned modulation of their toxicity and specificity. These results support the feasibility of this novel hypothesis.

StnI and StnII are two of the best well studied actinoporins and also constitute an optimum example of two almost identical isoforms (they share 91.0% of amino acid sequence identity) produced by the same sea anemone species but showing very different hemolytic activities (24,47,50,76). Consequently, they were the model proteins chosen to study the possibility of molecularly different actinoporins assembling into the same functional pore structure. Indeed, the employment of independently produced and isolated recombinant protein species excludes artifacts produced by traces of cross-contamination in the experiments shown that were made with only one single protein component.

Actinoporins pore-structure and stoichiometry is still highly controversial and far from being solved (22,36,66,69,70,77-79). The latest actinoporin pore-like oligomeric structure published is a crystalline octameric ensemble of FraC (66). According to those results, the two side-chain residues showing more buried surface upon oligomerization would be FraC Val60 and Trp149 (66,80). These residues have their corresponding counterparts in StnI (Ile 59 and Trp149) and StnII (Ile58 and Trp146). Both amino acids could nicely perform an identical function in the StnI-StnII mixed oligomers. Therefore, from a molecular point of view there would not be impediment for the formation of StnI-StnII heteropores.

Synergistic activity of StnI and StnII in both hemolysis and calcein-release experiments suggested that both proteins are in fact able to interact within the same pore structure (Figs. 1 to 3). Cross-linking experiments further support this observation since, and only in the presence of lipid vesicles, both StnI and StnII could be cross-linked with a short cross-linking agent (Figs. 4 and 5). Finally, we have also shown that mixtures of StnI and StnII show increased affinity for lipid vesicles, in agreement with the fact that both isoforms interact in the process of membrane binding and pore formation (Fig. 7). ITC and hemolytic experiments also show that 1.0% of StnII dramatically enhances StnI binding to lipid model vesicles driving a dramatic improvement of hemolytic activity. Taking into account the only moderate effects observed in calcein-leakage experiments, and the hemolysis results obtained with the two different StnII mutants used as control (Fig. 2), it can be also suggested that synergy between StnI and StnII could be mostly due to a better interaction with the membrane while the final step of pore formation would not be strongly affected.

As stated above, actinoporins represent multigene families. However, only two or three different isoforms are usually produced by the same sea anemone species in enough amount as to be detected and purified. For example, up to 19 different cDNA sequences have been detected for *S. helianthus*, the sea anemone producing StnI and StnII (43). Thus, taking into account this discrepancy between the number of actinoporin encoding genes found in sea anemones and the amount and diversity of isotoxins made, it is tempting to speculate that the less represented isoforms might play a role in regulating and/or

potentiating the activity and specificity of those ones produced in larger amount. Maybe this is just a strategy to fulfill a much more modulated and specific cytotoxic action against potential prey and/or predators.

Conclusions

Overall, the results presented here show that two different actinoporins produced by the same sea anemone species act in synergy, most probably interacting to form functional pores made of distinct protein isoforms. As far as we know, this observation has not been reported before. This interaction has sound consequences in terms of the biological functionality of actinoporins and suggests that it could represent a more general strategy employed by other pore forming proteins. According to the results reported now, it can be speculated that one of the reasons for actinoporins being multigene families is the possibility of interaction among different isotoxins to exert a much more modulated and/or potentiated action against their prey and/or predators. This possibility would translate into more versatile defense and/or attack responses in their natural environment.

Acknowledgements: The work was funded by grant BFU2012-32404 from the Spanish Ministerio de Ciencia e Innovación (JGG and AMP), an FPU fellowship granted to SGL, a UCM collaboration fellowship to ERT, and a Ramón y Cajal Award to JAC (RYC-2014-16604).

Conflict of interest: The authors declare that they have no conflicts of interest with the contents of this article.

Author contributions: ERT, SGL and JAC conducted the experiments. ERT, SGL, JAC, JL, JGG, and AMP conceived and designed the experiments, analyzed and discussed the results, wrote and corrected the manuscript, and suggested modifications.

.

REFERENCES

1. Maček, P. (1992) Polypeptide cytolytic toxins from sea anemones (*Actiniaria*). *FEMS Microbiol Immunol* **5**, 121-129
2. Anderluh, G., and Maček, P. (2002) Cytolytic peptide and protein toxins from sea anemones (Anthozoa: Actiniaria). *Toxicon* **40**, 111-124.
3. Alegre-Cebollada, J., Oñaderra, M., Gavilanes, J. G., and Martínez-del-Pozo, A. (2007) Sea anemone actinoporins: the transition from a folded soluble state to a functionally active membrane-bound oligomeric pore. *Curr Protein Pept Sci* **8**, 558-572
4. García-Ortega, L., Alegre-Cebollada, J., García-Linares, S., Bruix, M., Martínez-del-Pozo, A., and Gavilanes, J. G. (2011) The behavior of sea anemone actinoporins at the water-membrane interface. *Biochim Biophys Acta* **1808**, 2275-2288
5. Parker, M. W., and Feil, S. C. (2005) Pore-forming protein toxins: from structure to function. *Prog Biophys Mol Biol* **88**, 91-142
6. González, M. R., Bischofberger, M., Pernot, L., van der Goot, F. G., and Freche, B. (2008) Bacterial pore-forming toxins: the (w)hole story? *Cell Mol Life Sci* **65**, 493-507
7. Bischofberger, M., Iacovache, I., and van der Goot, F. G. (2012) Pathogenic pore-forming proteins: function and host response. *Cell Host Microbe* **12**, 266-275
8. Iacovache, I., van der Goot, F. G., and Pernot, L. (2008) Pore formation: An ancient yet complex form of attack. *Biochim Biophys Acta* **1778**, 1611-1623
9. Gouaux, E. (1997) Channel-forming toxins: Tales of transformation. *Current Opinion in Structural Biology* **7**, 566-573
10. Anderluh, G., Dalla Serra, M., Viero, G., Guella, G., Maček, P., and Menestrina, G. (2003) Pore formation by equinatoxin II, a eukaryotic protein toxin, occurs by induction of nonlamellar lipid structures. *J Biol Chem* **278**, 45216-45223.
11. Athanasiadis, A., Anderluh, G., Maček, P., and Turk, D. (2001) Crystal structure of the soluble form of equinatoxin II, a pore-forming toxin from the sea anemone *Actinia equina*. *Structure* **9**, 341-346
12. Kristan, K. C., Viero, G., Dalla Serra, M., Maček, P., and Anderluh, G. (2009) Molecular mechanism of pore formation by actinoporins. *Toxicon* **54**, 1125-1134
13. Gilbert, R. J. C., Dalla Serra, M., Froelich, C. J., Wallace, M. I., and Anderluh, G. (2014) Membrane pore formation at protein-lipid interfaces. *Trends Biochem Sci* **39**, 510-516
14. Hinds, M. G., Zhang, W., Anderluh, G., Hansen, P. E., and Norton, R. S. (2002) Solution structure of the eukaryotic pore-forming cytolysin equinatoxin II: Implications for pore formation. *J Mol Biol* **315**, 1219-1229.
15. Marchioretto, M., Podobnik, M., Dalla Serra, M., and Anderluh, G. (2013) What planar lipid membranes tell us about the pore-forming activity of cholesterol-dependent cytolysins. *Biophys Chem* **182**, 64-70
16. Rojko, N., Cronin, B., Danial, J. S., Baker, M. A., Anderluh, G., and Wallace, M. I. (2014) Imaging thelipid-phase-dependent pore formation of equinatoxin II in droplet interface bilayers. *Biophys J* **106**, 1630-1637
17. Rojko, N., Kristan, K. C., Viero, G., Zerovnik, E., Maček, P., Dalla Serra, M., and Anderluh, G. (2013) Membrane damage by an α-helical pore-forming protein,

Equinatoxin II, proceeds through a succession of ordered steps. *J Biol Chem* **288**, 23704-23715

18. Alegre-Cebollada, J., Rodríguez-Crespo, I., Gavilanes, J. G., and Martínez-del-Pozo, A. (2006) Detergent-resistant membranes are platforms for actinoporin pore-forming activity on intact cells. *FEBS J* **273**, 863-871
19. Castrillo, I., Araujo, N. A., Alegre-Cebollada, J., Gavilanes, J. G., Martínez-del-Pozo, A., and Bruix, M. (2010) Specific interactions of sticholysin I with model membranes: An NMR study. *Proteins* **78**, 1959-1970
20. García-Linares, S., Castrillo, I., Bruix, M., Menéndez, M., Alegre-Cebollada, J., Martínez-del-Pozo, A., and Gavilanes, J. G. (2013) Three-dimensional structure of the actinoporin sticholysin I. Influence of long-distance effects on protein function. *Arch Biochem Biophys* **532**, 39-45
21. García-Linares, S., Richmond, R., García-Mayoral, M. F., Bustamante, N., Bruix, M., Gavilanes, J. G., and Martínez-del-Pozo, A. (2014) The sea anemone actinoporin (Arg-Gly-Asp) conserved motif is involved in maintaining the competent oligomerization state of these pore-forming toxins. *FEBS J* **281**, 1465-1478
22. Mancheño, J. M., Martín-Benito, J., Martínez-Ripoll, M., Gavilanes, J. G., and Hermoso, J. A. (2003) Crystal and electron microscopy structures of sticholysin II actinoporin reveal insights into the mechanism of membrane pore formation. *Structure* **11**, 1319-1328
23. Alm, I., García-Linares, S., Gavilanes, J. G., Martínez-del-Pozo, A., and Slotte, J. P. (2015) Cholesterol stimulates and ceramide inhibits sticholysin II-induced pore formation in complex bilayer membranes. *Biochim Biophys Acta - Biomembranes* **1848**, 925-931
24. Valcarcel, C. A., Dalla Serra, M., Potrich, C., Bernhart, I., Tejuca, M., Martínez, D., Pazos, F., Lanio, M. E., and Menestrina, G. (2001) Effects of lipid composition on membrane permeabilization by sticholysin I and II, two cytolysins of the sea anemone *Stichodactyla helianthus*. *Biophys J* **80**, 2761-2774
25. Belmonte, G., Pederzolli, C., Maček, P., and Menestrina, G. (1993) Pore formation by the sea anemone cytolysin equinatoxin-II in red blood cells and model lipid membranes. *J Membr Biol* **131**, 11-22
26. Tejuca, M., Serra, M. D., Ferreras, M., Lanio, M. E., and Menestrina, G. (1996) Mechanism of membrane permeabilization by sticholysin I, a cytolysin isolated from the venom of the sea anemone *Stichodactyla helianthus*. *Biochemistry* **35**, 14947-14957
27. Shin, M. L., Michaels, D. W., and Mayer, M. M. (1979) Membrane damage by a toxin from the sea anemone *Stoichactis helianthus*. II. Effect of membrane lipid composition in a liposome system. *Biochim Biophys Acta* **555**, 79-88
28. De los Ríos, V., Mancheño, J. M., Lanio, M. E., Oñaderra, M., and Gavilanes, J. G. (1998) Mechanism of the leakage induced on lipid model membranes by the hemolytic protein sticholysin II from the sea anemone *Stichodactyla helianthus*. *Eur J Biochem* **252**, 284-289
29. Martínez, D., Otero, A., Álvarez, C., Pazos, F., Tejuca, M., Lanio, M. E., Gutiérrez-Aguirre, I., Barlič, A., Iloro, I., Arrondo, J. L., González-Mañas, J. M., and Lissi, E. (2007) Effect of sphingomyelin and cholesterol on the interaction of St II with lipidic interfaces. *Toxicon* **49**, 68-81

30. Alegre-Cebollada, J., Cunietti, M., Herrero-Galán, E., Gavilanes, J. G., and Martínez-del-Pozo, A. (2008) Calorimetric scrutiny of lipid binding by sticholysin II toxin mutants. *J Mol Biol* **382**, 920-930
31. Menestrina, G., Cabiaux, V., and Tejuca, M. (1999) Secondary structure of sea anemone cytolysins in soluble and membrane bound form by infrared spectroscopy. *Biochem Biophys Res Commun* **254**, 174-180
32. Pedrera, L., Gomide, A. B., Sánchez, R. E., Ros, U., Wilke, N., Pazos, F., Lanio, M. E., Itri, R., Fanani, M. L., and Álvarez, C. (2015) The presence of sterols favors sticholysin I-membrane association and pore formation regardless of their ability to form laterally segregated domains. *Langmuir* **31**, 9911-9923
33. Bakrač, B., and Anderluh, G. (2009) Molecular mechanism of sphingomyelin-specific membrane binding and pore formation by actinoporins. *Adv Exp Med Biol* **677**, 106-115
34. Barlič, A., Gutiérrez-Aguirre, I., Caaveiro, J. M., Cruz, A., Ruiz-Argüello, M. B., Pérez-Gil, J., and González-Mañas, J. M. (2004) Lipid phase coexistence favors membrane insertion of equinatoxin-II, a pore-forming toxin from *Actinia equina*. *J Biol Chem* **279**, 34209-34216
35. Caaveiro, J. M., Echabe, I., Gutiérrez-Aguirre, I., Nieva, J. L., Arrondo, J. L., and González-Mañas, J. M. (2001) Differential interaction of equinatoxin II with model membranes in response to lipid composition. *Biophys J* **80**, 1343-1353.
36. Wacklin, H. P., Bremec, B. B., Moulin, M., Rojko, N., Haertlein, M., Forsyth, T., Anderluh, G., and Norton, R. S. (2016) Neutron reflection study of the interaction of the eukaryotic pore-forming actinoporin equinatoxin II with lipid membranes reveals intermediate states in pore formation. *Biochim Biophys Acta* **1858**, 640-652
37. Bellomio, A., Morante, K., Barlič, A., Gutiérrez-Aguirre, I., Viguera, A. R., and González-Mañas, J. M. (2009) Purification, cloning and characterization of fragaceatoxin C, a novel actinoporin from the sea anemone *Actinia fragacea*. *Toxicon* **54**, 869-880
38. Monastyrnaya, M., Leychenko, E., Isaeva, M., Likhatskaya, G., Zelepuga, E., Kostina, E., Trifonov, E., Nurminski, E., and Kozlovskaya, E. (2010) Actinoporins from the sea anemones, tropical *Radianthus macrodactylus* and northern *Oulactis orientalis*: Comparative analysis of structure-function relationships. *Toxicon* **56**, 1299-1314
39. Monastyrnaya, M. M., Zykova, T. A., Apalikova, O. V., Shwets, T. V., and Kozlovskaya, E. P. (2002) Biologically active polypeptides from the tropical sea anemone *Radianthus macrodactylus*. *Toxicon* **40**, 1197-1217
40. Leichenko, E. V., Monastirnaya, M. M., Zelepuga, E. A., Tkacheva, E. S., Isaeva, M. P., Likhatskaya, G. N., Anastyuk, S. D., and Kozlovskaya, E. P. (2014) Hct-a is a new actinoporin family from the *Heteractis crispa* sea anemone. *Acta Naturae* **6**, 89-98
41. Hu, B., Guo, W., Wang, L. H., Wang, J. G., Liu, X. Y., and Jiao, B. H. (2011) Purification and characterization of gigantoxin-4, a new actinoporin from the sea anemone *Stichodactyla gigantea*. *Int J Biol Sci* **7**, 729-739
42. Anderluh, G., Barlič, A., Podlesek, Z., Maček, P., Pungercar, J., Gubensek, F., Zecchini, M. L., Serra, M. D., and Menestrina, G. (1999) Cysteine-scanning mutagenesis of an eukaryotic pore-forming toxin from sea anemone: topology in lipid membranes. *Eur J Biochem* **263**, 128-136

43. De los Ríos, V., Oñaderra, M., Martínez-Ruiz, A., Lacadena, J., Mancheño, J. M., Martínez-del-Pozo, A., and Gavilanes, J. G. (2000) Overproduction in *Escherichia coli* and purification of the hemolytic protein sticholysin II from the sea anemone *Stichodactyla helianthus*. *Protein Expr Purif* **18**, 71-76
44. Turk, T. (1991) Cytolytic toxins from sea anemones. *Toxin Reviews* **10**, 223-262
45. Wang, Y., Yap, L. L., Chua, K. L., and Khoo, H. E. (2008) A multigene family of *Heteractis* magnificalysins (HMgs). *Toxicon* **51**, 1374-1382
46. Anderluh, G., Krizaj, I., Strukelj, B., Gubensek, F., Maček, P., and Pungercar, J. (1999) Equinatoxins, pore-forming proteins from the sea anemone *Actinia equina*, belong to a multigene family. *Toxicon* **37**, 1391-1401
47. Álvarez, C., Mancheño, J. M., Martínez, D., Tejuca, M., Pazos, F., and Lanio, M. E. (2009) Sticholysins, two pore-forming toxins produced by the Caribbean sea anemone *Stichodactyla helianthus*: Their interaction with membranes. *Toxicon* **54**, 1135-1147
48. Del Monte-Martínez, A., González-Bacerio, J., Romero, L., Aragon, C., Martínez, D., Chávez, M. D., Álvarez, C., Lanio, M. E., Guisan, J. M., and Díaz, J. (2013) Improved purification and enzymatic properties of a mixture of sticholysin I and II: Isotoxins with hemolytic and phospholipase A activities from the sea anemone *Stichodactyla helianthus*. *Protein Expr Purif* **95C**, 57-66
49. Martínez, D., Morera, V., Álvarez, C., Tejuca, M., Pazos, F., García, Y., Raida, M., Padrón, G., and Eliana Lanio, M. (2002) Identity between cytolysins purified from two morphos of the Caribbean sea anemone *Stichodactyla helianthus*. *Toxicon* **40**, 1219.
50. Alegre-Cebollada, J., Clementi, G., Cunietti, M., Porres, C., Oñaderra, M., Gavilanes, J. G., and Martínez-del-Pozo, A. (2007) Silent mutations at the 5'-end of the cDNA of actinoporins from the sea anemone *Stichodactyla helianthus* allow their heterologous overproduction in *Escherichia coli*. *J Biotechnol* **127**, 211-221
51. Uechi, G. I., Toma, H., Arakawa, T., and Sato, Y. (2010) Molecular characterization on the genome structure of hemolysin toxin isoforms isolated from sea anemone *Actineria villosa* and *Phyllodiscus semoni*. *Toxicon* **56**, 1470-1476
52. Ros, U., Pedrera, L., Diaz, D., Karam, J. C., Sudbrack, T. P., Valiente, P. A., MartInez, D., Cilli, E. M., Pazos, F., Itri, R., Lanio, M. E., Schreier, S., and Avarez, C. (2012) The membranotropic activity of N-terminal peptides from the pore-forming proteins sticholysin I and II is modulated by hydrophobic and electrostatic interactions as well as lipid composition. *J Biosci* **36**, 781-791
53. Olivera, B. M., Rivier, J., Clark, C., Ramilo, C. A., Corpuz, G. P., Abogadie, F. C., Mena, E. E., Woodward, S. R., Hillyard, D. R., and Cruz, L. J. (1990) Diversity of *Conus* neuropeptides. *Science* **249**, 257-263
54. Alegre-Cebollada, J., Lacadena, V., Oñaderra, M., Mancheño, J. M., Gavilanes, J. G., and Martínez-del-Pozo, A. (2004) Phenotypic selection and characterization of randomly produced non-haemolytic mutants of the toxic sea anemone protein sticholysin II. *FEBS Lett* **575**, 14-18
55. Laemli, U. K. (1970) Cleavage of structural proteins during the assembly of the head of bacteriophage T4. *Nature* **227**, 680-685
56. Alegre-Cebollada, J., Martínez-del-Pozo, A., Gavilanes, J. G., and Goormaghtigh, E. (2007) Infrared spectroscopy study on the conformational changes leading to pore formation of the toxin sticholysin II. *Biophys J* **93**, 3191-3201

57. Pardo-Cea, M. A., Castrillo, I., Alegre-Cebollada, J., Martínez-del-Pozo, A., Gavilanes, J. G., and Bruix, M. (2011) Intrinsic local disorder and a network of charge-charge interactions are key to actinoporin membrane disruption and cytotoxicity. *FEBS J* **278**, 2080-2089
58. Martínez-Ruiz, A., García-Ortega, L., Kao, R., Lacadena, J., Oñaderra, M., Mancheño, J. M., Davies, J., Martínez-del-Pozo, A., and Gavilanes, J. G. (2001) RNase U2 and α-sarcin: A study of relationships. *Methods Enzymol* **341**, 335-351
59. Bartlett, G. R. (1959) Colorimetric assay methods for free and phosphorylated glyceric acids. *J Biol Chem* **234**, 469-471
60. Oñaderra, M., Mancheño, J. M., Lacadena, J., De los Ríos, V., Martínez-del-Pozo, A., and Gavilanes, J. G. (1998) Oligomerization of the cytotoxin α-sarcin associated with phospholipid membranes. *Mol Membr Biol* **15**, 141-144
61. Maula, T., Isaksson, Y. J., García-Linares, S., Niinivehmas, S., Pentikainen, O. T., Kurita, M., Yamaguchi, S., Yamamoto, T., Katsumura, S., Gavilanes, J. G., Martínez-del-Pozo, A., and Slotte, J. P. (2013) 2NH and 3OH are crucial structural requirements in sphingomyelin for sticholysin II binding and pore formation in bilayer membranes. *Biochim Biophys Acta* **1828**, 1390-1395
62. García-Linares, S., Alm, I., Maula, T., Gavilanes, J. G., Slotte, J. P., and Martínez-Del-Pozo, A. (2015) The effect of cholesterol on the long-range network of interactions established among sea anemone Sticholysin II residues at the water-membrane interface. *Mar Drugs* **13**, 1647-1665
63. De los Ríos, V., Mancheño, J. M., Martínez-del-Pozo, A., Alfonso, C., Rivas, G., Oñaderra, M., and Gavilanes, J. G. (1999) Sticholysin II, a cytolysin from the sea anemone *Stichodactyla helianthus*, is a monomer-tetramer associating protein. *FEBS Lett* **455**, 27-30
64. Pazos, I. F., Martínez, D., Tejuca, M., Valle, A., Martínez-del-Pozo, A., Álvarez, C., Lanio, M. E., and Lissi, E. A. (2003) Comparison of pore-forming ability in membranes of a native and a recombinant variant of Sticholysin II from *Stichodactyla helianthus*. *Toxicon* **42**, 571-578.
65. Maček, P., Belmonte, G., Pederzolli, C., and Menestrina, G. (1994) Mechanism of action of equinatoxin II, a cytolysin from the sea anemone *Actinia equina* L. belonging to the family of actinoporins. *Toxicology* **87**, 205-227
66. Tanaka, K., Caaveiro, J. M., Morante, K., González-Mañas, J. M., and Tsumoto, K. (2015) Structural basis for self-assembly of a cytolytic pore lined by protein and lipid. *Nat Commun* **6**, 6337
67. Cosentino, K., Ros, U., and García-Saez, A. J. (2015) Assembling the puzzle: Oligomerization of α-pore forming proteins in membranes. *Biochim Biophys Acta*
68. Ros, U., and García-Sáez, A. J. (2015) More than a pore: The interplay of pore-forming proteins and lipid membranes. *J Membr Biol* **248**, 545-561
69. Subburaj, Y., Ros, U., Hermann, E., Tong, R., and García-Sáez, A. J. (2015) Toxicity of an α-pore-forming toxin depends on the assembly mechanism on the target membrane as revealed by single-molecule imaging. *J Biol Chem* **290**, 4856-4865
70. Rojko, N., Dalla Serra, M., Maček, P., and Anderluh, G. (2016) Pore formation by actinoporins, cytolysins from sea anemones. *Biochim Biophys Acta* **1858**, 446-456

71. Martínez, D., Campos, A. M., Pazos, F., Álvarez, C., Lanio, M. E., Casallanovo, F., Schreier, S., Salinas, R. K., Vergara, C., and Lissi, E. (2001) Properties of St I and St II, two isotoxins isolated from *Stichodactyla helianthus*: a comparison. *Toxicon* **39**, 1547-1560.
72. Wong, E. S., and Belov, K. (2012) Venom evolution through gene duplications. *Gene* **496**, 1-7
73. Valle, A., Alvarado-Mesen, J., Lanio, M. E., Alvarez, C., Barbosa, J. A., and Pazos, I. F. (2015) The multigene families of actinoporins (part I): Isoforms and genetic structure. *Toxicon* **103**, 176-187
74. Brinkman, D. L., Konstantakopoulos, N., McInerney, B. V., Mulvenna, J., Seymour, J. E., Isbister, G. K., and Hodgson, W. C. (2014) *Chironex fleckeri* (box jellyfish) venom proteins: expansion of a cnidarian toxin family that elicits variable cytolytic and cardiovascular effects. *J Biol Chem* **289**, 4798-4812
75. Dewson, G. (2016) Doughnuts, daisy chains and crescent moons: the quest for the elusive apoptotic pore. *EMBO J* **35**, 371-373
76. Ros, U., Rodríguez-Vera, W., Pedrera, L., Valiente, P. A., Cabezas, S., Lanio, M. E., García-Saez, A. J., and Álvarez, C. (2015) Differences in activity of actinoporins are related with the hydrophobicity of their N-terminus. *Biochimie* **116**, 70-78
77. Martín-Benito, J., Gavilanes, F., de Los Ríos, V., Mancheño, J. M., Fernández, J. J., and Gavilanes, J. G. (2000) Two-dimensional crystallization on lipid monolayers and three-dimensional structure of sticholysin II, a cytolysin from the sea anemone *Stichodactyla helianthus*. *Biophys J* **78**, 3186-3194
78. Mechaly, A. E., Bellomio, A., Gil-Carton, D., Morante, K., Valle, M., González-Mañas, J. M., and Guerin, D. M. (2011) Structural insights into the oligomerization and architecture of eukaryotic membrane pore-forming toxins. *Structure* **19**, 181-191
79. Baker, M. A., Rojko, N., Cronin, B., Anderluh, G., and Wallace, M. I. (2014) Photobleaching reveals heterogeneous stoichiometry for equinatoxin II oligomers. *Chembiochem* **15**, 2139-2145
80. Morante, K., Caaveiro, J. M., Viguera, A. R., Tsumoto, K., and González-Mañas, J. M. (2015) Functional characterization of Val60, a key residue involved in the membrane-oligomerization of fragaceatoxin C, an actinoporin from *Actinia fragacea*. *FEBS Lett* **589**, 1840-1846

Table 1. Binding of StnI, StnII, or different StnI:StnII mixtures to DOPC:SM:Chol (1:1:1) vesicles studied by ITC. Thermodynamic parameters for protein mixtures StnI:StnII (95:5), StnI:StnII (90:10), and StnI:StnII (80:20) (Fig. 7) should be considered only as estimations and are shown only for trend consistency purposes because binding affinities were so high that keeping the *c* values within range involved dilutions below the recommended detection limits of the instrument. Therefore, the corresponding *c* values of the three mixtures containing the higher proportion of StnII are high above the recommended ones. Results shown are the average of at least three separate experiments.

	StnI:StnII (100:0)	**StnI:StnII (0:100)[a]**	**StnI:StnII (99:1)**	**StnI:StnII (95:5)**	**StnI:StnII (90:10)**	**StnI:StnII (80:20)**
n	49±1	39 ±4	38±1	42±1	38±1	47±9
K_a (M^{-1}) x 10^{-8}	0.41±0.03	1.70±0.90	2.84±0.91	33.90±41.90	23.20±19.90	237.00±29.30
ΔG (kcal/mol)	-8.21±0.03	-9.10±0.50	-10.90±0.48	-10.89±0.48	-10.73±0.37	-11.54±1.29
ΔH (kcal/mol)	-20.9±2.1	-44.0±3.0	-9.1±0.1	-11.1±0.1	-14.0±0.1	-27.3±3.2
ΔS (cal/mol·K)	-42.84±6.78	-115±9.00	-1.2±0.73	-0.8±2.0	-14.0±1.7	-52.9±6.4
[Protein]	10.0 μM	1.5 μM	1.5 μM	1.5 μM	1.5 μM	1.0 μM
***c*=K_a x [Protein]**	410	255	426	5090	3480	23700
RBM[b]	0.19	1.00	1.71	5.50	4.20	115.7

[a] (30).

[b] Relative membrane binding $[n_{(StnII)} \times K_{(other)}]/[n_{(other)} \times K_{(StnII)}]$ as explained in (30).

The abbreviations used are: 6HStnII, sticholysin II tagged wit six histidine residues at the amino-terminus; CD, circular dichroism; DMSO, dimethyl sulfoxide; DOPC, 1,2-dioleoyl-sn-glycero-3-phosphocholine; DSS, disuccinimidyl suberate; EqtII, equinatoxin II; ITC, isothermal titration calorimetry; LUV, large unilamellar vesicle; PFT, pore forming toxin; POC, phosphocholine; RMB, relative membrane binding; SD, standard deviation; SM, sphingomyelin; Stn, sticholysin.

FIGURE LEGENDS

FIGURE 1. (*Left panel*) Maximum hemolytic rate values (expressed as percentage of hemolysis per second) are represented versus the logarithm of total protein concentration: StnI (white dots), StnII (black dots), and the StnI:StnII (80:20) mixture (black squares). The white squares line was obtained as the arithmetical addition of the rates obtained with the individual proteins for the real concentration of each one in the different mixtures employed. Results shown are the average of four independently performed experiments. Each of these experiments was made by duplicate. Error bars represent ±SD. (*Right panel*) As a representative example, the hemolytic activity curves of StnI (white dots), StnII (black dots), or a StnI:StnII (80:20) mixture (black squares), at a total protein concentration of 2 nM, are also shown.

FIGURE 2. Maximum hemolytic rate values (expressed as percentage of hemolysis per second) are represented versus the logarithm of total protein concentration of individual and two different actinoporin mixtures: Wild-type StnI and A10PS28P (A) or Y111N (B) StnII mutants. In both panels it is shown the behavior of StnI (white dots), the StnII mutant (black dots), and the StnI:StnII mutant (80:20) mixture (black squares). The white squares line was obtained as the arithmetical addition of the rates obtained with the individual proteins for the real concentration of each one in the different mixtures employed. Results shown are the average of four independently performed experiments. Each of these experiments was made by duplicate. Error bars represent ±SD.

FIGURE 3. (*Left panel*) Calcein release maximal rates (expressed as normalized fluorescence intensity increment per second) are represented versus the total protein concentration: StnI (white dots), StnII (black dots), and the StnI:StnII (80:20) mixture (black squares). The white squares line was obtained as the arithmetical addition of the rates obtained with the individual proteins taking into account the real concentration of each one of them in the different mixtures employed. Results shown are the average of three independently performed experiments. Each of these experiments was made by duplicate. Error bars represent ±SD. (*Right panel*) As a representative example, the calcein leakage traces of StnI (white dots), StnII (black dots), or a StnI:StnII (80:20) mixture (black squares), at a total protein concentration of 5 nM, are also shown.

FIGURE 4. Immunoblotting detection of 6HStnII previously incubated in the presence, or not, of wild-type StnI**,** DOPC:SM:Chol (1:1:1) phospholipid vesicles, and/or DSS, as indicated. Proteins were detected using a mouse monoclonal anti-poly-Histidine-peroxidase antibody. The amount of 6HStnII loaded was 2.5 pmol. The StnI:6HStnII molar ratio employed was 80:20 in all instances shown. Molecular weight standards (EZ-RUN^{TM} pre-stained Rec Protein Ladder) were also loaded and the corresponding molecular masses are indicated in KDa at the left side margin of the figure.

FIGURE 5. Coomassie Blue stained gel (*upper panel*) and the corresponding immunoblotting detection (*lower panel*) of 6HStnII titrated with increasing amount of StnI are shown. The proteins, and also the mixtures assayed, were incubated in the presence, or not, of wild-type StnI**,** DOPC:SM:Chol (1:1:1) phospholipid vesicles, and/or DSS, as indicated. Proteins were detected using a mouse monoclonal anti-poly-Histidine-peroxidase antibody. The amount of 6HStnII loaded was 2.5 pmol in all instances shown. The StnI:6HStnII molar ratio employed is also indicated.

Molecular weight standards (EZ-RUN^{TM} pre-stained Rec Protein Ladder) were also loaded and the corresponding molecular masses are indicated in KDa at the left side margin of the figure.

FIGURE 6. Binding of StnI and StnII to DOPC:SM:Chol (1:1:1) vesicles studied by ITC. Reactant concentrations were those ones shown in Table 1. Binding isotherms were adjusted to a model in which protein membrane binding involves the participation of "n" lipid molecules (30). The *c* values ($c = K_a \times P_0$) for the graphs shown were within the range 1–1000.

FIGURE 7. Binding of StnI, StnII, and different StnI:StnII mixture (molar ratios as indicated) to DOPC:SM:Chol (1:1:1) vesicles studied by ITC. Reactant concentrations for the examples shown were P_0 = 1.5 μM and L_0 = 0.85 mM for all experiments shown, where P_0 refers to the initial total protein concentration within the calorimeter cell and L_0 is the lipid concentration within the dispensing auto-pipette. Binding isotherms were adjusted to a model in which protein membrane binding involves the participation of "n" lipid molecules (30). The *c* values ($c = K_a \times P_0$) for the graphs shown were in the 1–1000 range only for the StnI:StnII (0:100), StnI:StnII (99:1), and StnI:StnII (100:0). In the other three thermograms shown binding affinities were so high that keeping the *c* values within range involved dilutions below the recommended detection limits of the instrument.

FIGURE 8. (*Left panel*) Maximum hemolytic rate values (expressed as percentage of hemolysis per second) are represented versus the logarithm of total protein concentration of StnI (white dots) and an StnI:StnII (99:1) mixture (black squares). In these experiments the amount of StnII present in all the mixtures was so low that, when assayed in the absence of StnI, its hemolytic activity was undetectable in the time range measured. Results shown are the average of four independently performed experiments. Each of these experiments was made by duplicate. Error bars represent ±SD. (*Right panel*) As a representative example, the hemolytic activity curves of StnI at 3.96 nM (white dots), StnII at 0.04 nM (black dots) and the corresponding StnI:StnII (99:1) 4 nM mixture (black squares) are also shown.

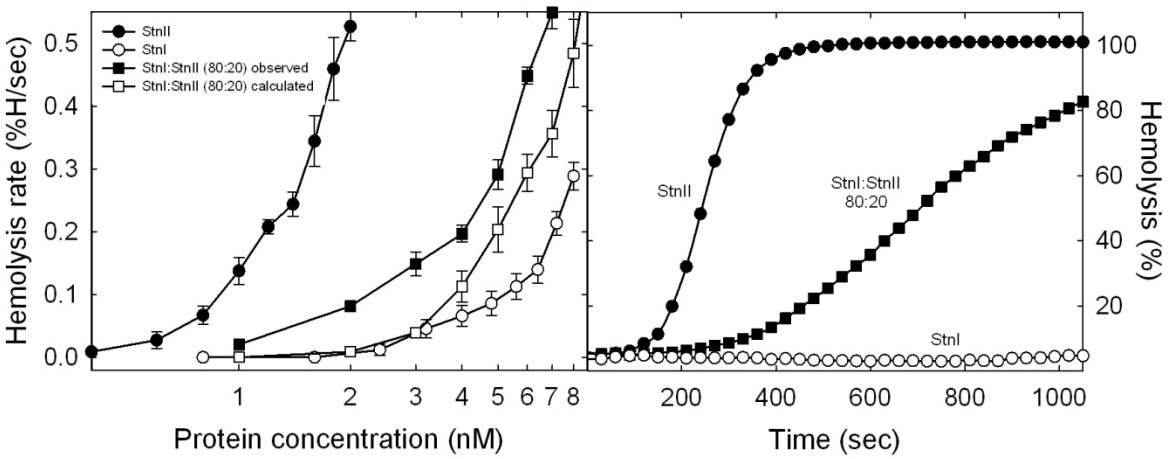
StnII
StnI
StnI:StnII (80:20) observed
StnI:StnII (80:20) calculated
Hemolysis rate (%H/sec)
0.0
0.1
0.2
0.3
0.4
0.5
1
2
3
4
5
6
7
8
Protein concentration (nM)
StnII
StnI:StnII
80:20
StnI
200
400
600
800
1000
Time (sec)
20
40
60
80
100
Hemolysis (%)

Figure 1

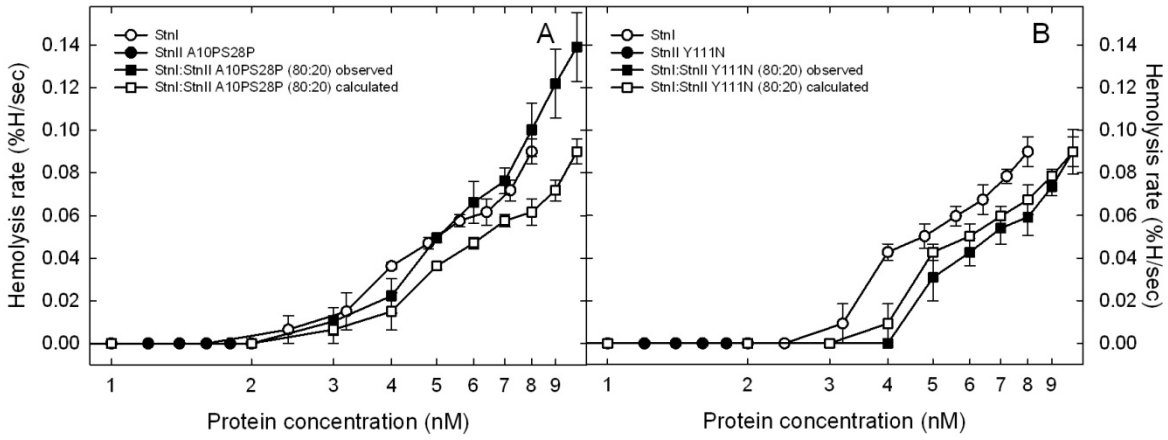
A
StnI
StnII A10PS28P
StnI:StnII A10PS28P (80:20) observed
StnI:StnII A10PS28P (80:20) calculated
Hemolysis rate (%H/sec)
Protein concentration (nM)
B
StnI
StnII Y111N
StnI:StnII Y111N (80:20) observed
StnI:StnII Y111N (80:20) calculated
Hemolysis rate (%H/sec)
Protein concentration (nM)

Figure 2

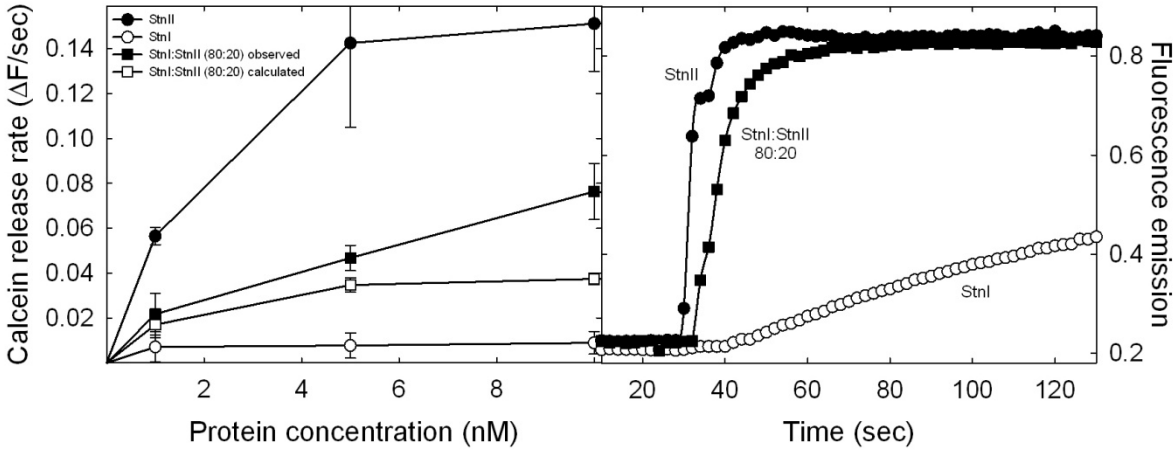
StnII
StnI
StnI:StnII (80:20) observed
StnI:StnII (80:20) calculated
Calcein release rate (ΔF/sec)
0.14
0.12
0.10
0.08
0.06
0.04
0.02
2
4
6
8
Protein concentration (nM)
StnII
StnI:StnII
80:20
StnI
0.8
0.6
0.4
0.2
20
40
60
80
100
120
Time (sec)
Fluorescence emission

Figure 3

	1	2	3	4	5	6
StnI (80)	+	+	+	+	-	+
6HStnII (20)	+	+	+	+	+	-
Vesicles	-	-	+	+	+	+
Cross-linker	-	+	-	+	+	+

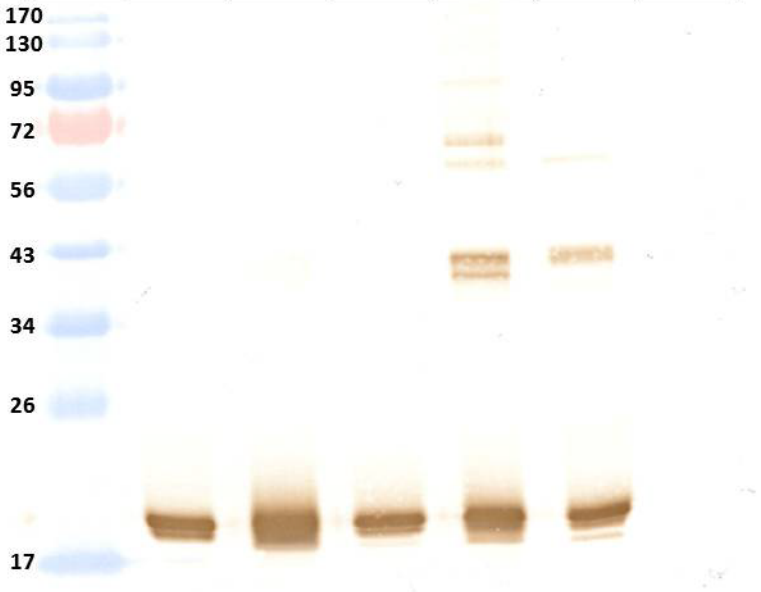

Figure 4

	1	2	3	4	5	6
StnI (pmol)	0.0	0.0	10.0	22.5	47.5	47.5
6HStnII (pmol)	2.5	2.5	2.5	2.5	2.5	0.0
StnI:6HStnII	0.0	0.0	80:20	90:10	95:5	-
Vesicles	-	+	+	+	+	-
Cross-linker	-	+	+	+	+	-

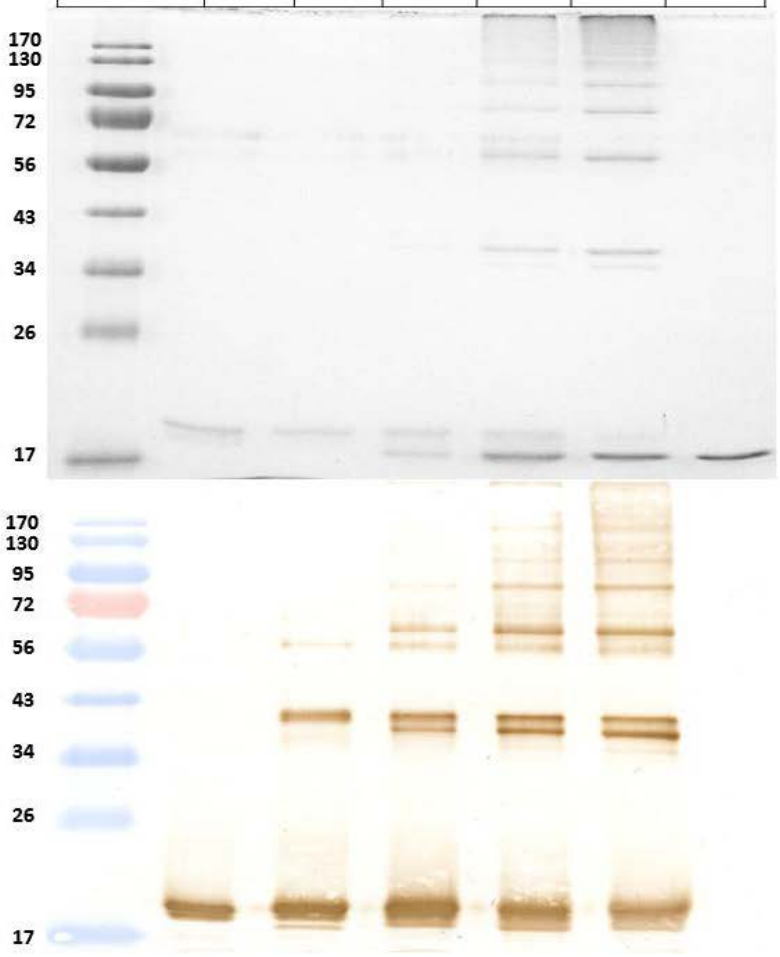

Figure 5

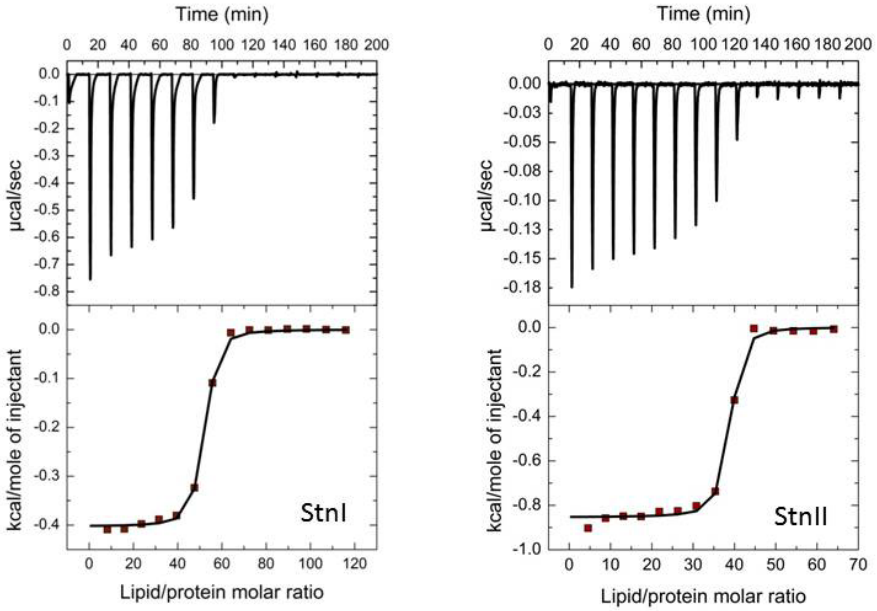
Time (min)
µcal/sec
kcal/mole of injectant
Lipid/protein molar ratio
StnI
Time (min)
µcal/sec
kcal/mole of injectant
Lipid/protein molar ratio
StnII

Figure 6

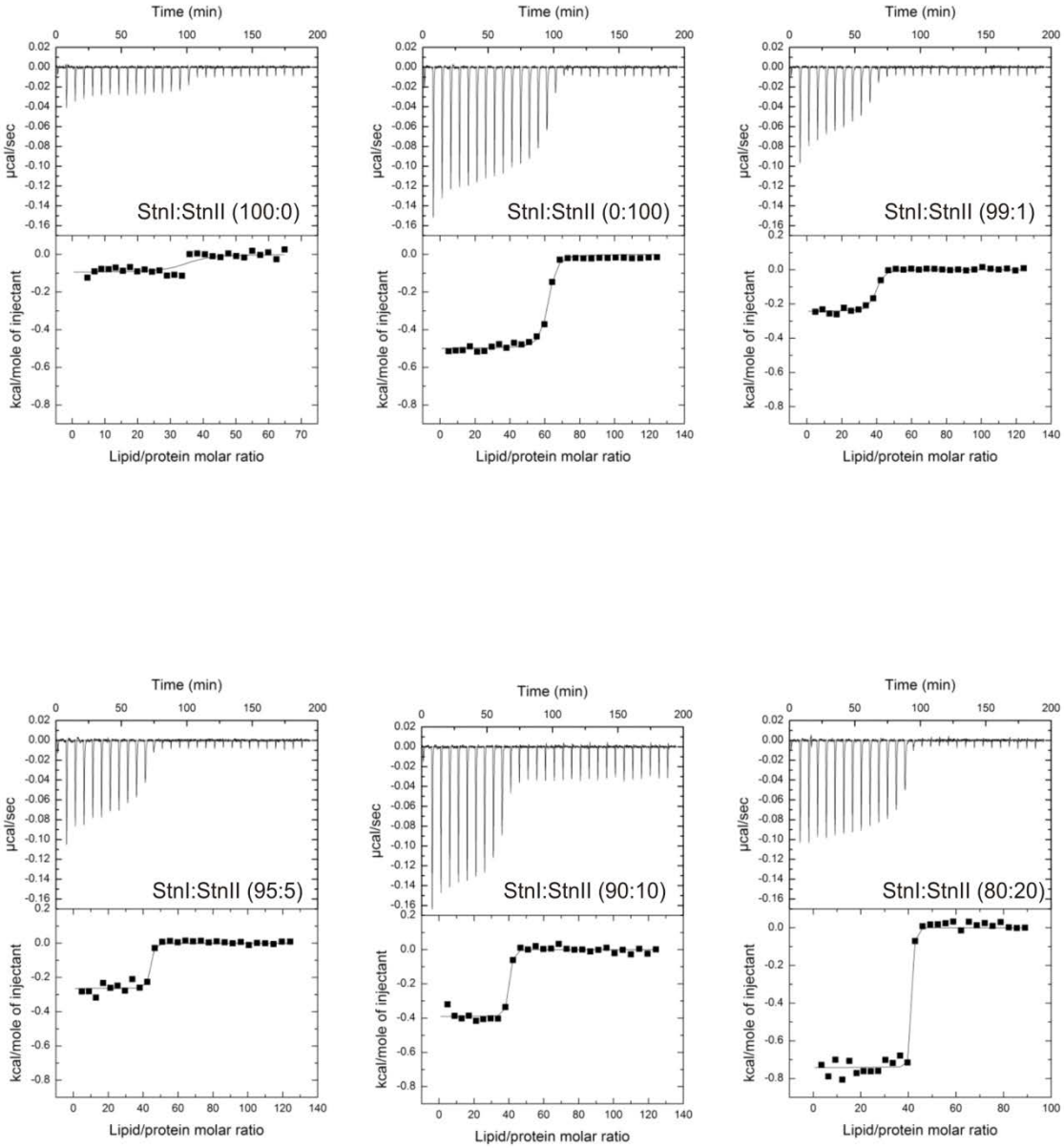
Time (min)
µcal/sec
StnI:StnII (100:0)
kcal/mole of injectant
Lipid/protein molar ratio
StnI:StnII (0:100)
StnI:StnII (99:1)
StnI:StnII (95:5)
StnI:StnII (90:10)
StnI:StnII (80:20)

Figure 7

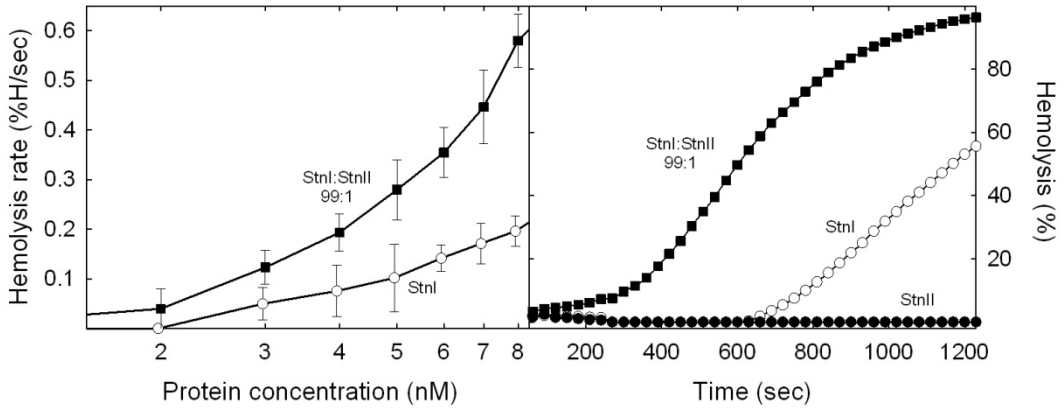
Hemolysis rate (%H/sec)
0.6
0.5
0.4
0.3
0.2
0.1
StnI:StnII
99:1
StnI
2
3
4
5
6
7
8
Protein concentration (nM)
200
400
600
800
1000
1200
Time (sec)
80
60
40
20
Hemolysis (%)
StnI:StnII
99:1
StnI
StnII

Figure 8